Deformation and Strength of Anisotropic Sand Under Three Dimensional Stress Conditions

by

Hidetoshi OCHIAI*, Yoshihiko TANABASHI* and Hiroyuki ISHIBASHI**

The three-dimensional, drained stress-strain and strength behavior of a sand prepared in cubical specimens with cross-anisotropic fabric was studied using triaxial compression, plane strain, and cubical triaxial tests with independent control of the three principal stresses. All specimens were loaded under conditions of principal stress directions fixed and aligned with the directions of the material axes. For comparable test conditions, the major principal strain was smallest and the rate of dilation was highest when the major principal stress acted perpendicular to the long axes of the sand grains. The opposite extremes were obtained when the major principal stress acted parallel to the long grain axes. The effects of initial cross-anisotropic fabric were mainly observed in the prefailure stress-strain behavior, whereas sufficient changes in the fabric had occurred at large strains to produce failure conditions which resembled those observed for isotropic sands. The three-dimensional failure surface could for practical purposes be modeled by an isotropic failure criterion.

Introduction

Natural in-situ sand deposits display fabric anisotropy due to parallel alignment of particles[1]. Several experimental studies have shown that fabric anisotropy may have considerable influence on the stress-strain and strength behavior of sand[1)~5)]. It has also been reported that the intermediate principal stress influences the stress-strain and strength behavior of initially isotropic sand deposits[6)]. The intermediate principal stress may have a similar influence on the behavior of sand with anisotropic fabric. Only a limited number of investigations of the three-dimensional behavior of anisotropic sand have been performed, and the available data are not always consistent.

Presented herein is an experimental study of the influence of the intermediate principal stress on the three-dimensional behavior of sand with anisotropic fabric under conditions of fixed and coinciding directions of material and principal stress axes. The testing procedure involved preparation of saturated, cubical specimens with strong preferred particle orientation like in a natural sand deposit. These specimens were temporarily frozen in order to facilitate their installation and desired orientation in the testing apparatus.

Received Jan. 1, 1983
*Department of Civil Engineering
**Graduate Student, Department of Civil Engineering

Drained tests were performed on these specimens using triaxial compression and plane strain equipment as well as cubical triaxial equipment with independent control of the three principal stresses.

Characterization of Sand, Specimen Preparation and Fabric

Sand Composition. - All tests in this study were performed on uniformly graded sand with particle sizes between 2.0 mm and 0.84 mm sieves. The specific gravity of grains was 2.708, and the maximum and minimum void ratios were 0.80 and 0.51, respectively.

The three principal dimensions of the sand particles, i. e. length, width and height, were studied using two microscopes. A grain was placed in its most stable position at the edge of a table and measured in vertical and horizontal directions through the two microscopes. Results based on the study of 250 particles are shown in Fig. 1 (a). The results are presented as length to height ratios, L/H, and length to width ratios, L/W, and they indicate that the sand grains are somewhat long and flat. According to previous studies[2] of several natural sands, typical values of axial ratio, which may include both W/L and H/L (no distinction was made between the two ratios), range from 0.5 to 0.7 corresponding to L/W and/or L/H ratios from 2.0 to 1.4. The sand selected for the present study is therefore representative of common natural sands, possibly with axial ratios in the upper end of the range.

Specimen Preparation. - Cubical specimens with side length of 76 mm were prepared in a specially designed mold by pouring and shaking sand grains in several layers. The specimen was then frozen in the mold, which was designed to avoid any expansion or disturbance of the sand structure during freezing.

A specimen was prepared in the mold in 10 layers. Each layer consisted of approximately 80 g of sand, which wax poured into de-aired water in the mold. The

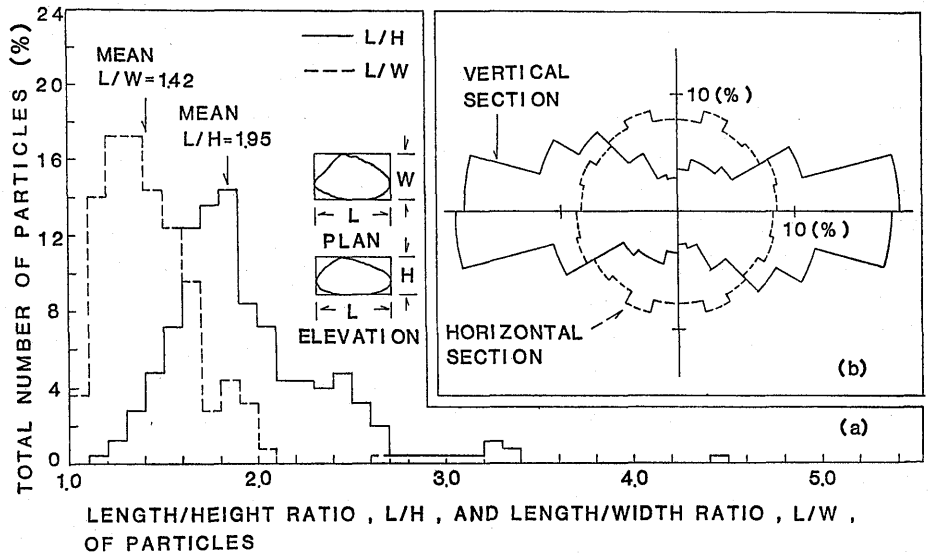

Fig. 1 (a) Grain shape distributions and (b) Rose diagrams of particle long axis orientations for specimens

mold was then placed on a vibrator and shaken for one minute by horizontal movements evenly distributed in all directions.

Specimen prepared by this method had void ratios of 0.53-0.54 corresponding to relative densities of 93-90 %.

Fabric Characterization. - In order to examine the fabric of a specimen, photographs were taken of horizontal and vertical sections through central regions of the specimen. This could be accomplished by melting part of a frozen specimen. The central region was used to avoid effects of the side walls which may locally have influenced the fabric. Measurements of orientation were made on photographic enlargements. The orientations of apparent long axes in horizontal and vertical sections of a specimen are shown on the rose diagram in Fig. 1 (b). In this study the orientations of 280 particles were measured for each section, and the orientation of each particle was assigned to one of the 15-degree intervals between 0 and 180 degrees. Fig. 1 (b) shows that the particles in the specimen prepared by the method described above had strong preferred orientations in the vertical section, but almost completely random orientations in the horizontal section. The specimen fabric is, therefore, of the cross-anisotropic type with a vertical axis of rotational symmetry and horizontal planes of isotropy.

Representation of Stresses and Strains

In order to present results of tests on anisotropic materials, it is important to clearly indicate the directions of stress and strain relative to the principal axes of the material. For this purpose a Cartesian coordinate system is employed as indicated in Fig.2. The X-axis coincides with the axis of rotational symmetry for the cross-anisotropic specimens. Stresses and strains are labeled according to this coordinate system.

The angle θ, indicated on the octahedrel plane in Fig. 2 (b) and (c), is measured clockwise from the σ_x-axis to the stress point P (σ_x, σ_y, σ_z) and is calculated as follows:

$$\tan\theta = \sqrt{3}\,\frac{\sigma_y-\sigma_z}{(\sigma_x-\sigma_y)+(\sigma_x-\sigma_z)} \qquad (1)$$

Values of θ are indicated on the stress axes in Fig. 2 (c).

The relative magnitude of the intermediate principal stress has often been indicated by the value of $b=(\sigma_2-\sigma_3)/(\sigma_1-\sigma_3)$. The paramater b is zero for triaxial compression in which $\sigma_2=\sigma_3$, and it is unity for triaxial extension in which $\sigma_2=\sigma_1$; for intermediate values of σ_2 the value of b is between zero and unity.

It is clear that the value of θ is sufficient to indicate the relative magnitudes of the principal stresses, and it also provides information regarding which of the normal stresses are the major, intermediate, and minor principal stresses. The value of b varies from 0 to 1 in each of the six sectors of the octahedral plane. However, the parameter b has frequently been used in studies of three-dimensional behavior of soils and it is convenient to use this parameter together with the parameter θ in the discussions of the test results presented below

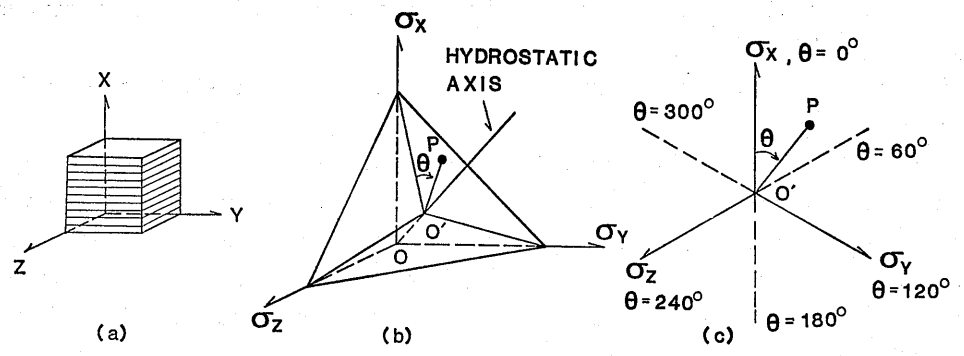

Fig. 2 Orientation of cross-anisotropic specimen relative to (a) Cartesian coordinate system, (b) Principal stress space, and (c) Octahedral plane

Testing Program and Procedures

Drained tests were performed under triaxial compression, plane strain, and cubical triaxial conditions. Constant effective confining pressure, σ'_3, of 0.50, 1.00, 2.00, and 4.00 kg/cm^2 were used in the triaxial compression tests, whereas the plane strain tests were performed with σ'_3=2.00 kg/cm^2. The effective confining pressure was 1.00 kg/cm^2 in all cubical triaxial tests.

The cubical triaxial tests were performed with constant values of b, i. e. the horizontal and vertical stress differences were increased proportionally until the specimen failed. A sufficient number of tests was performed to establish the three-dimensional failure surface under conditions of fixed directions of the principal stresses. These directions were aligned with the material axes as indicated in Fig. 2. Because the sand specimens were prepared with cross-anisotropic fabric, the three-dimensional failure surface in the octahedral plane was expected to be symmetric with regard to the X-axis in Fig. 2.

The major principal stress was applied in the vertical direction in all tests. Therefore, for θ-values in the range from 60° to 180°, the test specimens were rotated 90° relative to their orientation during preparation. All tests were strain controlled with a vertical strain rate slightly below 0.1 %/min.

Following installation, the frozen specimen was allowed to melt under an effective confining pressure of 0.20 kg/cm^2. To help saturate the specimens, a back pressure of 2.00 kg/cm^2 was applied to the triaxial compression and plane strain specimens, whereas a back pressure of 1.00 kg/cm^2 was employed for the cubical triaxial specimens. Measured values of $B=\triangle u/\triangle\sigma_3$ ranged between 0.94 and 0.99, which, for the relatively stiff sand specimens, correspond to sufficiently high degrees of saturation to perform reliable drained tests.

Stress-Strain and Volume Change Characteristics

Triaxial Compression. - Fig. 3 shows the stress-strain and volume change behavior obtained from the triaxial compression tests. The differences in behavior between tests at θ=0° and θ=120° are clearly reflected for all applied confining pressures. For given

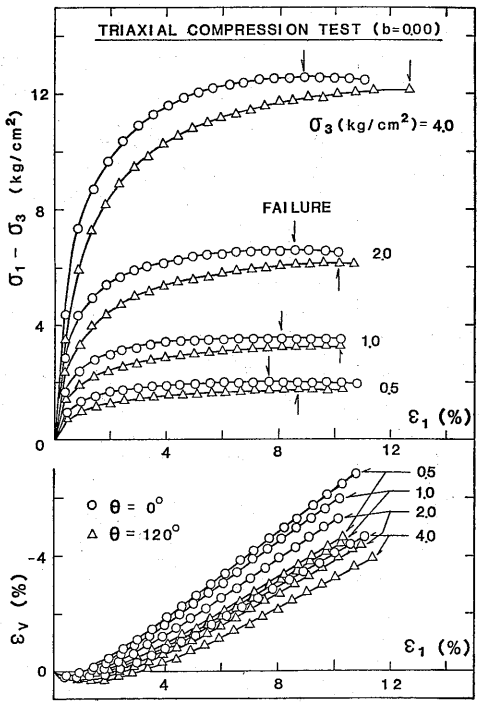

Fig. 3 Stress-strain and volume change characteristics obtained in triaxial compression tests on a sand with cross-anisotropic fabric

low to medium values of stress difference the compressive strains, ε_1, perpendicular to the long axes of the grains ($\theta=0°$) are about half of the compressive strains parallel to the long axes of the grains ($\theta=120°$). As failure is approached at large strains the stress-strain curves tend to approach each other, and the differences in friction angles in the triaxial compression tests shown in Fig. 3 are about 2° for $\sigma_3=0.50$ kg/cm² and only about 0.5° for $\sigma_3=4.00$ kg/cm².

The strain-to-failure is smaller in the tests with $\theta=0°$ than in the tests with $\theta=120°$, but the ratios of strain-to-failure are closer to unity than the ratios of strain observed at lower stress levels in the tests with $\theta=0°$ and $\theta=120°$. Thus, it appears that the effects of the initial anisotropic fabric are substantially diminished at large strains.

This may be because remolding and re-orientation of grains have resulted in fabrics within the specimens loaded at $\theta=0°$ and $\theta=120°$ which are more alike and to lesser degrees resemble the original anisotropic fabric.

The volumetric strain behavior also reflects the initial anisotropic fabric of the specimens. Thus, the specimens loaded at $\theta=0°$ exhibit smaller amounts of initial compression and larger rates of dilation than those loaded at $\theta=120°$. However, the volumetric strain pattern does not reflect fabrics which become more alike at large strains, as discussed above.

The overall comparison between the triaxial compression tests loaded at $\theta=0°$ and at $\theta=120°$ resembles a comparison between tests on dense (corresponds to $\theta=0°$) and loose (corresponds to $\theta=120°$) sand performed at high confining pressures. Thus, the dense sand exhibits higher initial modulus, less initial compression and higher rate of dilation, lower strain-to-failure, and only slightly higher strength than does the loose sand tested at the same high confining pressure.

Tests with Three Unequal Principal Stresses. - The stress-strain and volume change behavior observed in the cubical triaxial tests performed with constant b-values and the behavior obtained from the plane strain tests are shown in Fig. 4. The results from two triaxial compression tests are also shown in Fig. 4 for comparison. Because the plane strain tests were performed with $\sigma'_3=2.00$ kg/cm², and the other tests were performed with $\sigma'_3=1.00$ kg/cm², the normalized stress differences, $(\sigma_1-\sigma_3)/\sigma'_3$, are plotted versus the major principal strain, ε_1, in Fig. 4. The relative magnitudes of the intermediate principal stress is indicated by the value of b, whereas the directions of the principal stresses relative to the specimen orientation is indicated by the value of θ.

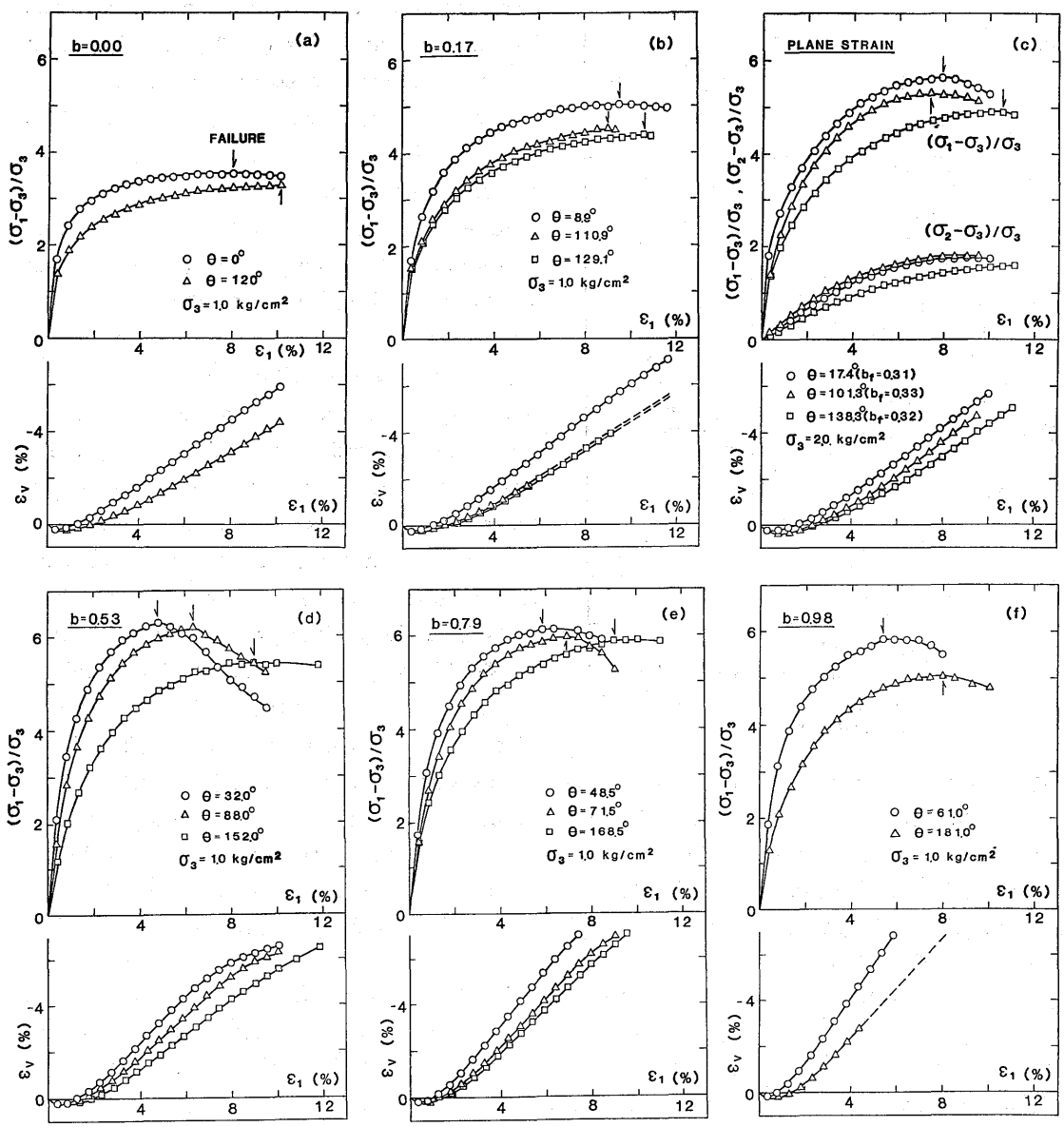

Fig. 4 Stress-strain and volume change characteristics obtained in cubical triaxial and plane strain tests on a sand with cross-anisotropic fabric

For each value of b and given values of stress difference, the compressive strains, ε_1, are smallest and the rates of dilation, $-\Delta\varepsilon_V/\Delta\varepsilon_1$, are highest for $0° \leq \theta \leq 60°$, intermediate behavior is observed for $60° \leq \theta \leq 120°$, and ε_1-values are larger and values of $-\Delta\varepsilon_V/\Delta\varepsilon_1$ are lowest for $120° \leq \theta \leq 180°$. Although the value of b is not constant in plane strain tests, this behavior pattern is the same for these tests as for the tests with constant b-values. The strain-to-failure does not always follow this pattern, especially for low b-values where the stress-strain curves are rather flat. The sequence is, however, clearly followed for higher b-values where the strain-to-failure is better defined from the more pronounced peak failure points.

Strengh Characteristics

The variations of the measured friction angles with the value of b are shown in Fig. 5 for each of the three 60-degree sectors of θ. In each of these sectors, the friction angle is smallest for b=0.00 and it increases initially with increasing magnitude of the intermediate principal stress until the value of b reaches 0.50 to 0.75. The slight decrease in friction angle close to b=1.00 is observed in all three sectors of θ. This pattern in strength behavior is similar to that observed by Lade and Duncan[7] for Monterey No. 0 Sand.

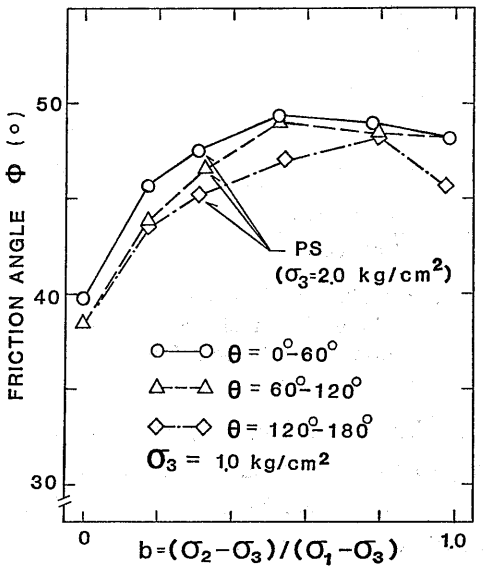

Fig. 5 Failure sutface shown in ϕ-b diagram for cubical triaxial and plane strain tests on a sand with cross-anisotropic fabric

Fig. 5 also shows that the largest difference in friction angle between the three sectors of θ occurs at b=1.00, where $\Delta\phi = 2.6°$. Because the variations in friction angle shown on Fig. 5 are quite consistent and follow the sequence of the three θ-sectors discussed above, the maximum difference in friction angle of 2.6° observed for dense sand cannot be considered as scatter in the test results. However, this difference may not be inportant from a practical point of view. Anisotropic sands with smaller strain-to-failure may, however, exhibit larger differences in strengths, because of the smaller amounts of remolding and reoreintation of grains occurring in response to smaller local shear deformations.

The shape of the failure surface indicated in Fig. 5 may be modeled to some degree by the following three-dimensional failure criterion proposed by Lade[8]:

$$f_p = (I_1^3/I_3 - 27)\ (I_1/p_a)^m \qquad (2a)$$

$$f_p = \eta_1 \quad \text{at failure} \qquad (2b)$$

in which I_1 and I_3 are the first and the third stress invariants defined as follows in terms of principal stresses :

$$I_1=\sigma_1+\sigma_2+\sigma_3 \qquad (3)$$

$$I_3=\sigma_1 \cdot \sigma_2 \cdot \sigma_3 \qquad (4)$$

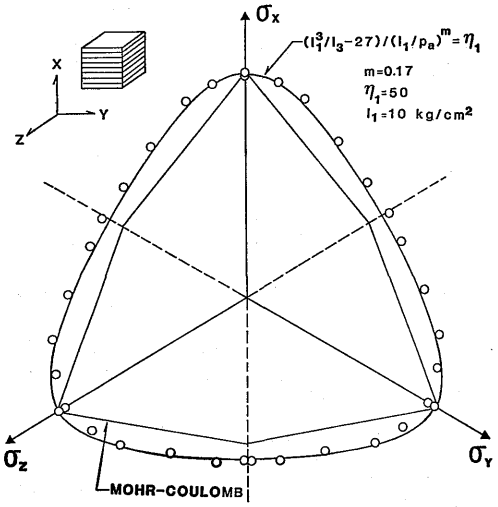

Fig. 6 Failure surface shown in octahedral plane for tests on a sand with cross-anisotropc fabric

and p_a is atmospheric pressure expressed in the same units as the stresses. The parameters η_1 and m are constants, whose values may be determined from triaxial compression tests.

Sand specimens with cross-anisotropic fabric obtained from the field would most likely have vertical axes of material symmetry, and they would be installed in the apparatus and loaded in triaxial compression at $\theta=0°$ (see Fig. 2). The results of the triaxial compression tests on a sand corresponding to $\theta=0°$ were therefore used for determiation of material parameters. Values of $\eta_1=50$ and $m=0.17$ were obtained as explained in ref. (8). The cross-section of the corresponding failure surface is shown in the octahedral plane for which $I_1=10\,kg/cm^2$ as seen in Fig. 6. The experimental failure points have been projected on the same octahedral plane for comparison with the isotropic failure surface expressed by Eq. (2). The failure surface of the cross-anisotropic sand is expected to be symmetric with regard to the σ_x-axis, and the experimental points obtained for $0° \leqq \theta \leqq 180°$ were therefore also shown in the region of $180° \leqq \theta \leqq 360°$. The failure criterion in Eq. (2) describes the experimentally obtained failure surface with good accuracy. The largest difference occurs at $\theta=60°$ (and $\theta=300°$), where the measured friction angle is about 3° higher than that calculated from Eq. (2). The Mohr-Coulomb failure criterion fitted to the tests at $\theta=0°$ is also shown on Fig. 6. It may be seen that the failure criterion expressed in Eq. (2) describes the strength characteristics of a sand with initially anisotropic fabric quite accurately as compared to the Mohr-Coulomb failure criterion.

Directions of Strain Increment Vectors

It is of interest to study the directions of plastic strain increment vectors relative to the yield or failure surface in the principal stress space, because it may be possible to model the stress-strain behavior by plasticity theory. For this purpose the principal srtain increment axes are superimposed on the stress axes in the principal stress space. Only the directions of the strain increment vectors at failure will be considered. All

strain increments are plastic at failure, because the changes in stress at failure are negligible, thus resulting in negligible elastic strain incremrnts. The directions of the strain increment vectors are calculated from the slopes of the relations between the principal strains.

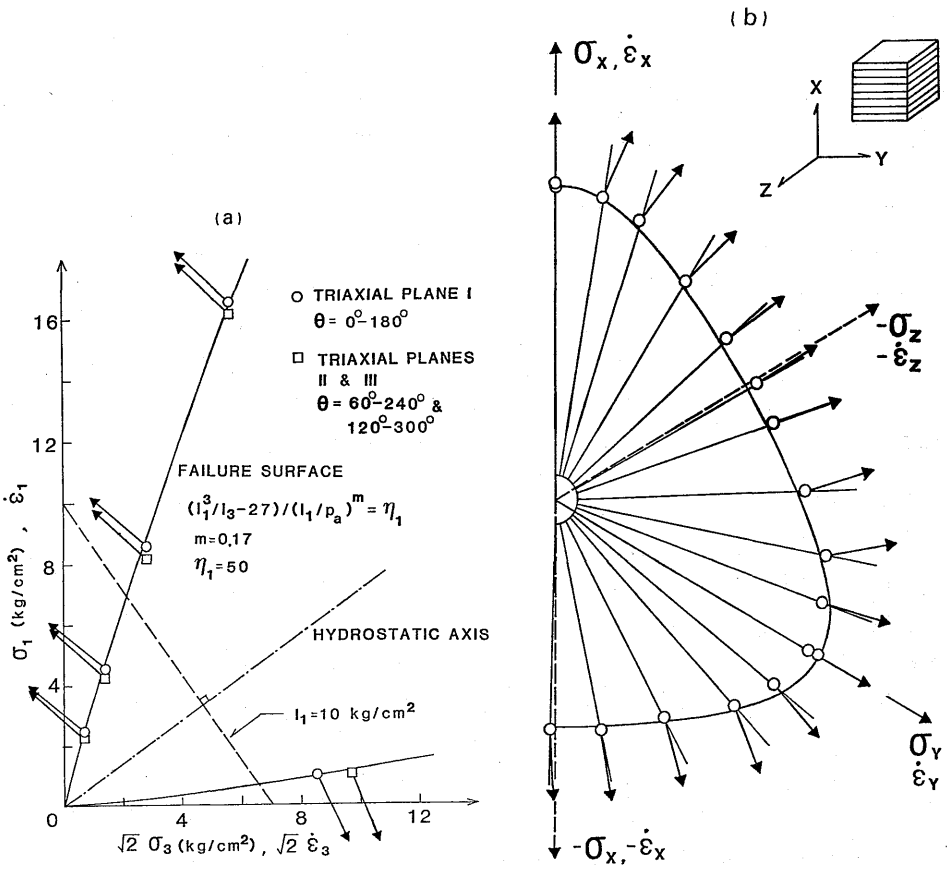

Fig. 7 Directions of projected strain increment vectors in (a) Triaxial planes, and in (b) Octahedral plane for a sand with cross-anisotropic fabric

Triaxial Planes. - There are three triaxial planes in the principal stress space, each containing one of the principal stress axes. For a material with cross-anisotropic properties, two of the triaxial planes are expected to show coinciding results. Thus, only two triaxial planes need be considered in evaluation of materials with cross-anisotropic properties.

The directions of the strain increment vectors corresponding to two different triaxial planes are projected on these planes and shown initiating from the respective failure stress points in Fig. 7 (a). The trace of the failure surface given by Eq. (2) is also shown in Fig. 7 (a). As previously observed for isotropic sand[7], the strain increment vectors are not perpendicular to the failure surface, and the normality condition from classical

plasticity theory is therefore not satisfied. It may be seen, however, that the directions of the strain increment vectors in the two triaxial planes are almost parallel at similar states of stress. The slight differences in directions relate to the different rates of dilation discussed above.

Octahedral Plane. - Projected directions of strain increment vectors are shown on the octahedral plane in Fig. 7 (b) together with the failure stress points and the failure surface calculated from Eq. (2). Only one half of the octahedral plane is shown, because of symmetry in material behavior as discussed in relation to Fig. 2.

It may be seen from Fig. 7 (b) that the strain increment vectors are nearly perpendicular to the failure surface in the octahedral plane. They are also for practical purposes symmetric with regard to the projected stress axes.

Observations similar to those presented above were also made with regard to the behavior of isotropic sand[7]. Thus, it appears that the effect of the initial cross-anisotropic fabric of the sand specimens has to a large extent been eliminated at failure, which occurred at relatively large strains in the tests on the sand. The general pattern of the directions of the plastic strain increment vectors relative to the failure surface is of importance in considerations regarding the applicability of plasticity theory and the general framework required for modeling of sand with anisotropic fabric.

Conclusions

The three-dimensional stress-strain and strength behavior of a sand prepared in cubical specimens with cross-anisotropic fabric was studied using triaxial compression, plane strain, and cubical triaxial tests with independent control of the three principal stresses. The cubical triaxial tests were performed with constant values of $b=(\sigma_2-\sigma_3)/(\sigma_1-\sigma_3)$.

Specimens consisting of relatively long, flat sand grains were prepared with strong preferred grain crientations in vertical sections and almost completely random orientations in horizontal sections. A sufficient number of tests was performed on these cross-anisotropic specimems to establish the three-dimensional failure surface and the stress-strain behavior under conditions of principal stress directions fixed and aligned with the directions of the material axes.

The results of both isotropic compression tests and shear tests indicate that the compressibility is smallest in the direction perpendicular to the long axes of the sand grains. Within each of three sectors in the principal stress space, the initial modulus increased, the rate of dilation increased and the strain-to-failure decreased with increasing value of b. Comparison of results from each of the three sectors indicated definite effects of the initial cross-anisotropic fabric on the prefailure stress-strain and volume change behavior. For each value of b and given values of stress difference, the major principal strain was smallest and the rate of dilation was highest when the major principal stress acted perpendicular to the long axes of the sand grains. A gradual variation in this behavior was observed as the state of stress was changed through the other two sectors.

The sand behavior at failure was only slightly affected by the initial cross-anisotropic

fabric. Thus, the experimentally obtained three-dimensional failure surface could for practical purposes be modeled by an isotropic failure criterion. Similarly, the directions of the plastic strain increment vectors superimposed on the principal stress space resembled those obtained for isotropic sand.

In summary, the effects of the initial cross-anisotropic fabric were mainly observed in the prefailure stress-strain behavior of the sand, whereas sufficient changes in the fabric had occured at large strains to produce failure conditions which resembled those observed for isotropic sands.

Refferences

1) Oda, M. (1972) : Soils and Foundations, Vol. 12, No. 1, pp. 17-36.
2) Oda,M., Koshigawa, I. and Higuchi, T. (1978) : Soils and Foundations, Vol 18, No. 1, pp. 25-38.
3) Matsuoka, H. and Ishizaki, H. (1981) : Proc. 10th ICSMFE, Vol. 1, pp. 669-702.
4) Yamada, Y. and Ishihara, K. (1979) : Soils and Foundations, Vol. 19, No. 2, pp. 79-94.
5) Arthur, J. R. F. and Menzies, B. K. (1972) : Geotechnique, Vol. 22, No. 1, pp. 115-128.
6) Ko, H. Y. and Scott, R. F. (1968) : Jour. of ASCE, Vol. 94, No. SM 4, pp. 883-898.
7) Lade, P. V. and Duncan, J. M. (1973) : Jour. of ASCE, Vol. 99, No. SM 10, pp. 793-812.
8) Lade, P. V. (1977) : Int. Jour. of Solids and Structures, Pergamon Press, Vol. 13, pp. 1019-1035.